AIP | Review of Scientific Instruments

Hard X-ray nanofocusing using adaptive focusing optics based on piezoelectric deformable mirrors

Takumi Goto, Hiroki Nakamori, Takashi Kimura, Yasuhisa Sano, Yoshiki Kohmura, Kenji Tamasaku, Makina Yabashi, Tetsuya Ishikawa, Kazuto Yamauchi, and Satoshi Matsuyama

Citation: Review of Scientific Instruments **86**, 043102 (2015); doi: 10.1063/1.4916617
View online: http://dx.doi.org/10.1063/1.4916617
View Table of Contents: http://scitation.aip.org/content/aip/journal/rsi/86/4?ver=pdfcov
Published by the AIP Publishing

Hard X-ray nanofocusing using adaptive focusing optics based on piezoelectric deformable mirrors

Takumi Goto,[1] Hiroki Nakamori,[1] Takashi Kimura,[2] Yasuhisa Sano,[1] Yoshiki Kohmura,[3] Kenji Tamasaku,[3] Makina Yabashi,[3] Tetsuya Ishikawa,[3] Kazuto Yamauchi,[1,4,5] and Satoshi Matsuyama[1,a)]

[1]*Department of Precision Science and Technology, Graduate School of Engineering, Osaka University, 2-1 Yamada-oka, Suita, Osaka 565-0871, Japan*
[2]*Research Institute for Electronic Science, Hokkaido University, Kita 21 Nishi 10, Kita-ku, Sapporo 001-0021, Japan*
[3]*SPring-8/RIKEN, 1-1-1 Kouto, Sayo, Hyogo 679-5198, Japan*
[4]*Center for Ultra-Precision Science and Technology, Graduate School of Engineering, Osaka University, 2-1 Yamada-oka, Suita, Osaka 565-0871, Japan*
[5]*CREST, JST, 2-1 Yamada-oka, Suita, Osaka 565-0871, Japan*

(Received 2 October 2014; accepted 15 March 2015; published online 2 April 2015)

An adaptive Kirkpatrick–Baez mirror focusing optics based on piezoelectric deformable mirrors was constructed at SPring-8 and its focusing performance characteristics were demonstrated. By adjusting the voltages applied to the deformable mirrors, the shape errors (compared to a target elliptical shape) were finely corrected on the basis of the mirror shape determined using the pencil-beam method, which is a type of at-wavelength figure metrology in the X-ray region. The mirror shapes were controlled with a peak-to-valley height accuracy of 2.5 nm. A focused beam with an intensity profile having a full width at half maximum of 110 × 65 nm (V × H) was achieved at an X-ray energy of 10 keV. © *2015 AIP Publishing LLC.* [http://dx.doi.org/10.1063/1.4916617]

I. INTRODUCTION

Third-generation synchrotron radiation facilities and X-ray free-electron lasers can generate X-ray beams with high intensity and high coherence. A focused beam allows researchers to efficiently perform X-ray analysis with high spatial resolution and high sensitivity, and in such facilities, various types of X-ray focusing devices based on reflection,[1,2] refraction,[3] and diffraction[4,5] techniques are used to provide nanofocused beams. Focus sizes of less than 50 nm have been attained with ultraprecise focusing devices.

Generally, X-ray focusing devices are specially designed and fabricated for specific purposes. They usually have fixed optical parameters such as focal length and numerical aperture. Recently, however, deformable mirrors that can actively control such optical parameters by freely adjusting their shapes have attracted considerable attention. They enable researchers to perform various experiments without changing focusing devices and, if necessary, to simultaneously compensate for wavefront errors introduced by other optics. Various types of deformable mirrors based on mechanical actuators[6–8] and piezoelectric actuators[9–11] have been reported.

In this paper, we focus on the development of ultraprecise deformable mirrors based on piezoelectric actuators and deformation control through the pencil-beam method,[12,13] which is a type of at-wavelength figure metrology in the X-ray region. We aim to achieve diffraction-limited nanofocusing using an adaptive focusing system. In addition, a precise deformation procedure that uses *ex-situ* and *in-situ* figure metrologies is proposed. Ultraprecise deformable mirrors are developed by eliminating the inherent waviness on the mirror substrates through elastic emission machining,[14] and a high-magnification X-ray beam monitor is specially developed to improve the pencil-beam method. Under testing, the deformation errors of the deformable mirrors, defined as the height errors from a target elliptical shape after deformation of the shape, are finely corrected *in situ* to yield a figure accuracy of 2.5 nm; this satisfies the Rayleigh quarter-wavelength criterion. In addition, X-rays with 10-keV energy focused by the two mirrors, which are aligned in the Kirkpatrick–Baez (KB) configuration, are characterized in order to confirm that the mirrors function as ideal focusing optics.

II. PIEZOELECTRIC DEFORMABLE MIRROR

The developed deformable mirrors with piezoelectric bimorph structures consist of a single quartz glass substrate and 4 long piezoelectric actuators (Fig. 1).[15,16] In each mirror, four piezoelectric actuators are attached to the face and back of the substrate, two to the front and two to the back. The two piezoelectric actuators attached to the face have 18 electrodes that can be used to produce an arbitrary shape (Fig. 1(a)). In contrast, the two piezoelectric actuators attached to the back have a single electrode that controls the entire mirror curvature (Fig. 1(b)). By adjusting the two electrode groups, the target elliptical shape can be obtained. This division of the roles facilitates deformation to a target ellipse, because the figure error between the initial shape and the elliptical shape tends to consist of a major quadratic shape and minor high-order polynomial shapes. The electrode pattern with 5.6-mm pitch and only 0.8-mm space was produced using a magnetron

a)Author to whom correspondence should be addressed. Electronic mail: matsuyama@prec.eng.osaka-u.ac.jp

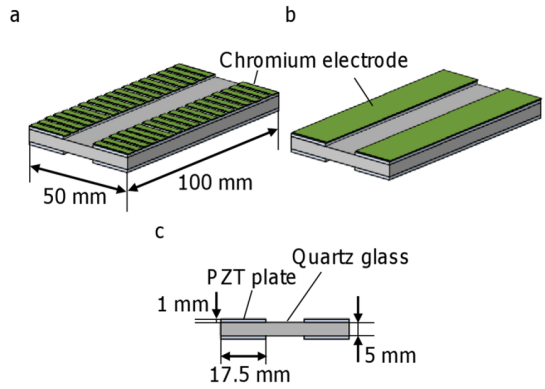

FIG. 1. Schematic of the (a) face side and (b) back side of the deformable mirror. (c) Cross-sectional view.

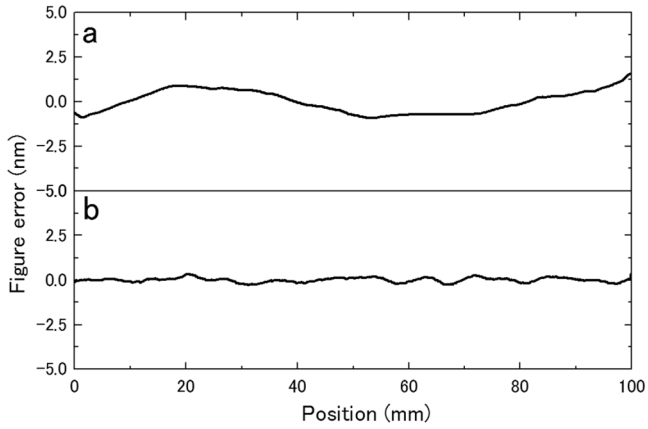

FIG. 2. Residual figure errors of the (a) horizontal and (b) vertical focusing mirrors. They were processed by subtracting an arbitrary quadratic shape from the shapes measured with an optical interferometer.

sputtering method. Moreover, to enable precise deformation, the intrinsic figure error of the substrate in the high-spatial-frequency range was removed through elastic emission machining. This is because a shape with shorter spatial wavelength than that of the electrode array cannot be produced by deformation. At this time, the figure error from an arbitrary quadratic shape was also removed, with a figure accuracy upwards of 3 nm, to facilitate deformation (Fig. 2). This is because the substrates had figure errors with relatively large curvature in local areas as well as high-spatial-frequency figure errors. Correcting the figure error with large curvature requires high-voltage power supplies; i.e., the adjustable curvature is limited by the maximum voltage of the power supply. Note that quadratic shape errors were ignored because they are easily and finely corrected by deformation using the piezoelectric actuator on the back side. According to our experiments, such a single electrode on a piezoelectric actuator can produce highly uniform curvature with a height error of at most 4 nm, which includes measurement errors of an optical interferometer (see the supplementary material Fig. 1(s).[17] After the fabrication process was completed, the effective area was covered with a 100-nm-thick platinum layer using a sputtering method.

III. DEFORMATION PROCEDURE

To precisely deform such a mirror to a given target elliptical shape, we propose the following deformation procedure. First, the shape is measured using an *ex-situ* optical interferometer (VeriFire XPZ, Zygo Corp.) and the figure error from the ellipse is corrected by deforming the mirror. The process is continued until the target shape is obtained. We continuously record all the voltage patterns applied to all the electrodes in a log file during the process. Next, in a synchrotron radiation facility, the mirror is deformed by applying the same voltage patterns on the basis of the log file to improve the reproducibility of the deformation, which would be degraded by hysteresis of the piezoelectric actuators if this process was omitted. Furthermore, to finely correct the deformation error, the applied voltages are adjusted *in situ* on the basis of the mirror shape obtained through the pencil-beam method. This method is advantageous as it consists of a simple setup without special instruments, demonstrates ease of use, and has the potential for automatic measurement along with a wide dynamic range for the measurement of figure errors.

Typically, ~20-μm X-ray beams passing through a slit placed immediately upstream of a mirror illuminate one section of the mirror surface. The reflected beam is detected using a beam monitor placed on the focus point. The process is repeated until the entire effective area is scanned using a stage under the slit. Then, by calculating the median point shift of the reflected beam, we obtain the slope error distribution over the scanned area. To improve the accuracy of this measurement, a high-magnification X-ray beam monitor was specially developed. It consists of a YAG:Ce ceramics scintillator of 50-μm thickness, a mirror, a lens (10X), and a CMOS camera (BITRAN, CS-52M, 2048 × 1536 pixels, 2.5 μm/pixel). The lens has a numerical aperture of 0.2, which has been optimized in relation to the scintillator thickness so that the beam monitor displays the optimal resolution.[18]

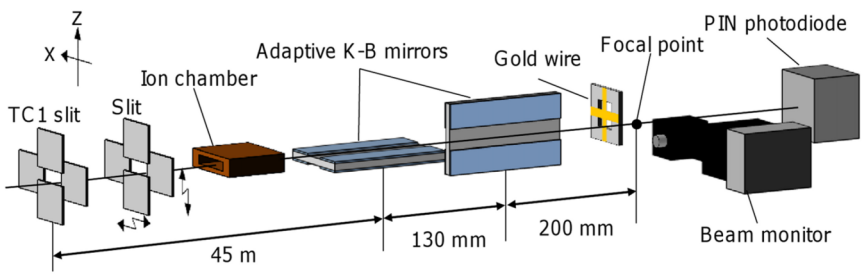

FIG. 3. Experimental setup of the deformable Kirkpatrick–Baez mirror focusing system.

TABLE I. Parameters of the designed ellipses.

	Horizontal focusing mirror	Vertical focusing mirror
a[a] (m)	22.600	22.665
b[a] (mm)	12.000	15.142
Grazing incidence angle[b] (mrad)	4	4
Focal length[c] (mm)	200	330
Maximum concave depth (μm)	14	8

[a]Ellipse: $x^2/a^2 + y^2/b^2 = 1$.
[b]Averaged over the whole area.
[c]At the center of the mirror.

IV. EXPERIMENTS AND RESULTS

To demonstrate almost fully diffraction-limited focusing using the ultraprecise deformable mirror and deformation control in combination, we constructed an adaptive two-dimensional focusing optical system, in which the two mirrors were aligned in a KB mirror arrangement,[19] at the third experimental hutch of the BL29XUL beamline at SPring-8. The X-ray energy used in all experiments was 10 keV and a schematic of the focusing system setup is shown in Fig. 3. Table I lists the parameters of the designed elliptical shape. The deformable mirrors were connected to multiple high-voltage power supplies that were developed by our group and which can supply voltages in the range of ±250 V with ripple voltages of 10 mV p-p. The incident slit and motorized XZ stages used for slit scanning were placed immediately upstream of the mirrors. The X-ray beam monitor and a gold cross wire of 200 μm in diameter were placed at the focus, and the latter was used to characterize the beam shape using the wire-scan method.

One of the most important factors for precisely adjusting the deformation of the mirror is the accuracy of the pencil-beam method. Therefore, before conducting the focusing test, we investigated the characteristics of this method, which utilizes

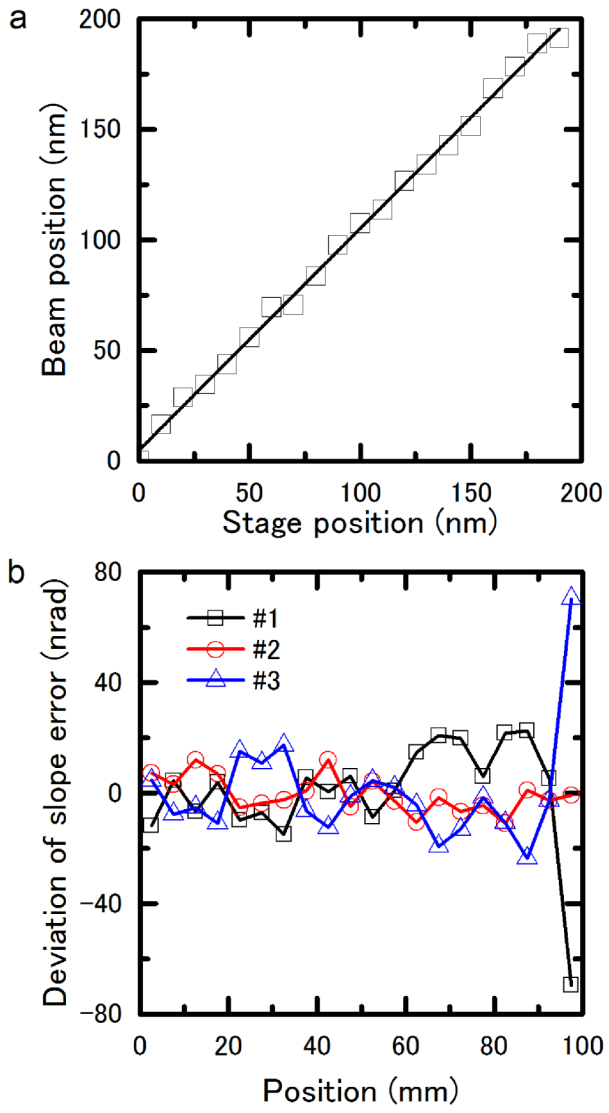

FIG. 4. Beam monitor performance. (a) Median point shift detection accuracy and (b) repeatability. Data for (a) were collected using a beam limited by a pinhole. The measurement in (b) was conducted three times using a focused beam with the deformable mirrors. The deviations from the averages of the three values were plotted.

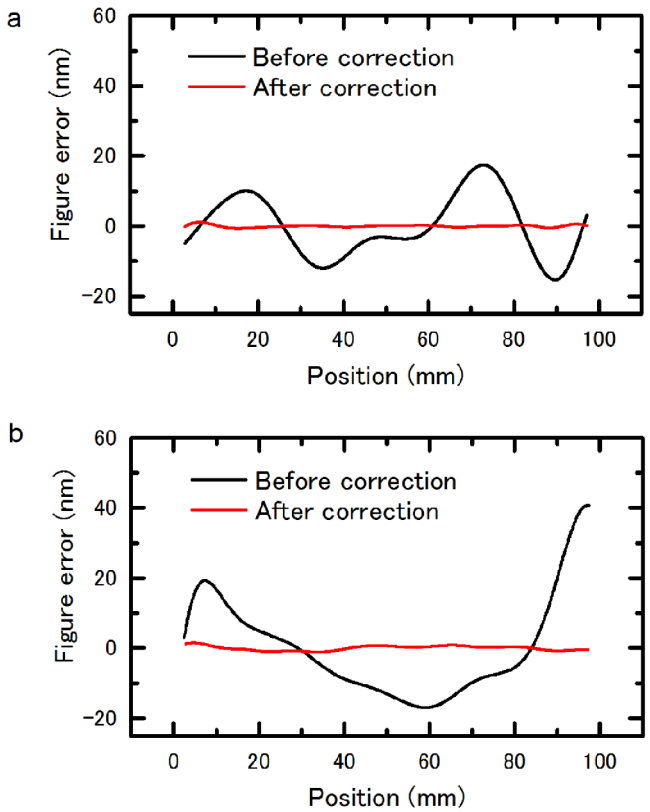

FIG. 5. Figure errors before and after final correction. (a) Horizontal and (b) vertical focusing mirrors. The reproducibility is less than 0.3 nm peak to valley (data not shown).

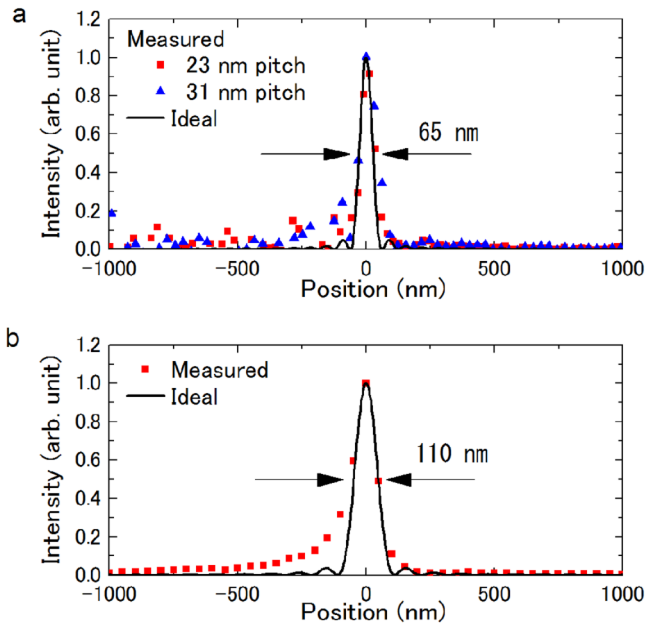

FIG. 6. Intensity profiles of the focused beam in the (a) horizontal and (b) vertical directions.

the developed beam monitor. To obtain the detection limit of the beam monitor that detects the median point shift of the X-ray beam, we used an X-ray beam limited by a nickel pinhole of 50-μm thickness and 20-μm diameter, rather than a focused beam. This is because this experiment requires very high stability with beam position variation of less than 5 nm. Generally, an X-ray focused by mirrors does not have sufficient stability at this level. The median points of the beam were measured by changing the pinhole position with a 10-nm pitch using motorized XZ stages (SIGMA TECH Co., LTD., FS-1050SPX) with a positioning accuracy of 1 nm. Fig. 4(a) shows the relationship between the pinhole position and the obtained median point of the beam, and demonstrates that the beam monitor can detect the beam position with an accuracy of ~10 nm. We also investigated the repeatability of the pencil-beam method using a focused beam with the two deformable mirrors as a practical test. We performed the pencil-beam scan three times while maintaining the voltages applied to the deformable mirrors. Fig. 4(b) shows the deviation of the slope errors measured at each section of the mirror. The pencil-beam method has a reproducibility of ~50 nrad for the practical condition. Thus, the pencil-beam method enables us to determine the figure error of the mirror with a figure accuracy of ~0.25 nm, which is estimated from the maximum slope error when this figure error shape is assumed to be a simple sine wave with an amplitude of 0.125 nm and spatial wavelength of 15 mm.

Prior to performing a two-dimensional focusing test, the mirrors were deformed by applying initial voltages that were predetermined as described above so as to produce the target elliptical shape. Then, to finely correct the deformation errors, we adjusted the applied voltages on the basis of the deformation error determined using the pencil-beam method. In the pencil-beam method, the slit width was set to 20 μm, which corresponds to 20 divisions of the mirror aperture. Slope errors were measured at 20 points on the mirror surface. The deformation error was calculated by integrating the slope errors after complementing the data using the spline interpolation algorithm. The procedure, which was automatically performed by our developed program, was repeated 40 times for the horizontal focusing mirror and 115 times for the vertical focusing mirror. Figure 5(a) shows the figure error of the horizontal focusing mirror before and after the fine correction. The figure error before the fine correction has a peak-to-valley height of 40 nm and, after the fine correction, the mirror could be deformed to the target elliptical shape with an accuracy of 2 nm. Fig. 5(b) shows the figure error of the vertical focusing mirror, and it can be seen that the peak-to-valley (PV) figure error was improved from 60 to 2.5 nm. After the fine correction, the beam intensity profiles at the focal point were measured, as shown in Fig. 6. A full width at half maximum (FWHM) of 110 nm (vertical, V) × 65 nm (horizontal, H) was achieved, which is in good agreement with the diffraction-limited FWHM of 98 nm (V) × 58 nm (H) for an X-ray energy of 10 keV. After measuring the intensity profiles, we performed the pencil-beam scan again for both directions. Consequently, drifting of the deformation was observed. The drift speed of the horizontal focusing mirror was 3 nm/h, which was obtained from the maximum error between the figure error before the beam profiling and the figure error after the beam profiling. By contrast, that of the vertical focusing mirror was 13 nm/h. This deformation drift can explain why the beam profiles have long tails, especially in the vertical direction; essentially, the focus beam appears to be gradually degrading because of the deformation drift.

V. CONCLUSION

We developed ultraprecise piezoelectric deformable mirrors and a precise deformation procedure based on *ex-situ* and *in-situ* figure metrologies. Hence, we achieved almost fully diffraction-limited X-ray nanofocusing using adaptive KB-mirror focusing optics, and have therefore improved the deformation procedure. In the near future, we will complete the development of a technique that allows fine corrections to be performed within an hour, which is ~10 times quicker than the fine correction process used in this experiment. In fact, such fine and quick correction has already been realized in *ex-situ* conditions, in which the fine correction is performed using an optical interferometer only. The resultant adaptive focusing system would allow us to effectively perform X-ray analysis and microscopy at various conditions without changing focusing optics. Furthermore, the adaptive focusing system would contribute to the development of multifunctional microscopy[20,21] that combines various X-ray analyses and microscopies.

ACKNOWLEDGMENTS

This research was supported by the JST CREST project. It was partially supported by JSPS KAKENHI (Grant No. 23226004) and the MEXT Global COE program (H08). The use of the BL29XUL beamline at SPring-8 was supported by RIKEN. We would like to acknowledge the JTEC Corporation for assistance with substrate processing.

[1]H. Mimura, H. Yumoto, S. Matsuyama, Y. Sano, K. Yamamura, Y. Mori, M. Yabashi, Y. Nishino, K. Tamasaku, T. Ishikawa, and K. Yamauchi, Appl. Phys. Lett. **90**, 051903 (2007).
[2]H. Mimura, S. Handa, T. Kimura, H. Yumoto, D. Yamakawa, H. Yokoyama, S. Matsuyama, K. Inagaki, K. Yamamura, Y. Sano, K. Tamasaku, Y. Nishino, M. Yabashi, T. Ishikawa, and K. Yamauchi, Nat. Phys. **6**, 122 (2009).
[3]C. G. Schroer, O. Kurapova, J. Patommel, P. Boye, J. Feldkamp, B. Lengeler, M. Burghammer, C. Riekel, L. Vincze, A. van der Hart, and M. Küchler, Appl. Phys. Lett. **87**, 124103 (2005).
[4]H. Yan, V. Rose, D. Shu, E. Lima, H. C. Kang, R. Conley, C. Liu, N. Jahedi, A. T. Macrander, G. B. Stephenson, M. Holt, Y. S. Chu, M. Lu, and J. Maser, Opt. Express **19**, 15069 (2011).
[5]T. Chen, Y. Chen, C. Wang, I. M. Kempson, Y. S. Chu, Y. Hwu, and G. Margaritondo, Opt. Express **19**, 19919 (2011).
[6]S. Yuan, M. Church, V. V. Yashchuk, K. A. Goldberg, R. S. Celestre, W. R. McKinney, J. Kirschman, G. Morrison, T. Noll, T. Warwick, and H. A. Padmore, X-Ray Opt. Instrum. **2010**, 784732.
[7]M. Idir, P. Mercere, M. H. Modi, G. Dovillaire, X. Levecq, S. Bucourt, L. Escolano, and P. Sauvageot, Nucl. Instrum. Methods **616**, 162 (2010).
[8]D. J. Merthe, V. V. Yashchuk, K. A. Goldberg, M. Kunz, N. Tamura, W. R. McKinney, N. A. Artemiev, R. S. Celestre, G. Y. Morrison, E. H. Anderson, B. V. Smith, and E. E. Domning, Opt. Eng. **52**(3), 033603 (2013).
[9]J. Susini, D. Labergerie, and L. Zhang, Rev. Sci. Instrum. **66**, 2229 (1995).
[10]R. Signorato, O. Hignette, and J. Goulon, J. Synchrotron Radiat. **5**, 797 (1998).
[11]T. Kimura, S. Handa, H. Mimura, H. Yumoto, D. Yamakawa, S. Matsuyama, K. Inagaki, Y. Sano, K. Tamasaku, Y. Nishino, M. Yabashi, T. Ishikawa, and K. Yamauchi, Jpn. J. Appl. Phys., Part 2 **48**, 2 (2009).
[12]O. Hignette, A. Freund, and E. Chinchio, Proc. SPIE **3152**, 188 (1997).
[13]J. P. Sutter, S. G. Alcock, and K. J. S. Sawhney, J. Synchrotron Radiat. **19**, 960 (2012).
[14]K. Yamauchi, H. Mimura, K. Inagaki, and Y. Mori, Rev. Sci. Instrum. **73**, 4028 (2002).
[15]H. Nakamori, S. Matsuyama, S. Imai, T. Kimura, Y. Sano, Y. Kohmura, K. Tamasaku, M. Yabashi, T. Ishikawa, and K. Yamauchi, Rev. Sci. Instrum. **83**, 053701 (2012).
[16]H. Nakamori, S. Matsuyama, S. Imai, T. Kimura, Y. Sano, Y. Kohmura, K. Tamasaku, M. Yabashi, T. Ishikawa, and K. Yamauchi, Nucl. Instrum. Methods Phys. Res., Sect. A **710**, 93 (2013).
[17]See supplementary material at http://dx.doi.org/10.1063/1.4916617 for the result of the deformation test when a piezoelectric deformable mirror with a single electrode was deformed.
[18]T. Martin and A. Koch, J. Synchrotron Radiat. **13**, 180 (2006).
[19]P. Kirkpatrick and A. V. Baez, J. Opt. Soc. Am. **38**, 766 (1948).
[20]S. Matsuyama, T. Kimura, H. Nakamori, S. Imai, Y. Sano, Y. Kohmura, K. Tamasaku, M. Yabashi, T. Ishikawa, and K. Yamauchi, Proc. SPIE **8503**, 850303 (2012).
[21]T. Kimura, S. Matsuyama, K. Yamauchi, and Y. Nishino, Opt. Express **21**, 9267 (2013).